Comparative Medicine
Copyright 2018
by the American Association for Laboratory Animal Science

Vol 68, No 4
August 2018
Pages 269–279

Original Research

Effect of Daytime Blue-enriched LED Light on the Nighttime Circadian Melatonin Inhibition of Hepatoma 7288CTC Warburg Effect and Progression

Robert T Dauchy,[1,*] Melissa A Wren-Dail,[1] Lynell M Dupepe,[2] Steven M Hill,[1] Shulin Xiang,[1] Muralidharan Anbalagan,[1] Victoria P Belancio,[1] Erin M Dauchy,[1] and David E Blask[1]

Liver cancer is the second leading cause of cancer death worldwide. Metabolic pathways within the liver and liver cancers are highly regulated by the central circadian clock in the suprachiasmatic nuclei (SCN). Daily light and dark cycles regulate the SCN-driven pineal production of the circadian anticancer hormone melatonin and temporally coordinate circadian rhythms of metabolism and physiology in mammals. In previous studies, we demonstrated that melatonin suppresses linoleic acid metabolism and the Warburg effect (aerobic glycolysis)in human breast cancer xenografts and that blue-enriched light (465–485 nm) from light-emitting diode lighting at daytime (bLAD) amplifies nighttime circadian melatonin levels in rats by 7-fold over cool white fluorescent (CWF) lighting. Here we tested the hypothesis that daytime exposure of tissue-isolated Morris hepatoma 7288CTC-bearing male rats to bLAD amplifies the nighttime melatonin signal to enhance the inhibition of tumor growth. Compared with rats housed under a 12:12-h light:dark cycle in CWF light, rats in bLAD light evinced a 7-fold higher peak plasma melatonin level at the mid-dark phase; in addition, high melatonin levels were prolonged until 4 h into the light phase. After implantation of tissue-isolated hepatoma 7288CTC xenografts, tumor growth rates were markedly delayed, and tumor cAMP levels, LA metabolism, the Warburg effect, and growth signaling activities were decreased in rats in bLAD compared with CWF daytime lighting. These data show that the increased nighttime circadian melatonin levels due to bLAD exposure decreases hepatoma metabolic, signaling, and proliferative activities beyond what occurs after normal melatonin signaling under CWF light.

Abbreviations: 13-HODE, 13-hydroxyoctadecadienoic acid; A–V, arterial–venous difference; bLAD, blue-enriched LED light at daytime; CWF, cool white fluorescent; ERK1/2, extracellular signal regulated kinase p44/46; FFA, free fatty acids; ipRGC, intrinsically photosensitive retinal ganglion cell; LA, linoleic acid; LED, light-emitting diode; SCN, suprachiasmatic nuclei; STAT3, signal transducer and activator of transcription 3; TFA, total fatty acids.

DOI: 10.30802/AALAS-CM-17-000107

Light influences circadian, neuroendocrine, and neurobehavioral regulation in all mammals.[2,3,8,13,31,41,47] The light–dark cycle entrains the master biologic clock, which is located in the suprachiasmatic nucleus (SCN) of the brain.[50] Residing within the eyes is a small set of retinal cells called the intrinsically photosensitive retinal ganglion cells (ipRGC), which contain the chromophore melanopsin; this protein mediates photobiologic responses in circadian rhythms of metabolism and physiology.[3,29,35,61] Melanopsin detects light quanta mostly in the blue-appearing portion of the visible spectrum (465 to 485 nm) in both humans and rodents, and the photic information is transmitted through the retinohypothalamic tract to the SCN.[15,29,35,53] The SCN controls the daily pineal gland production of the circadian neurohormone melatonin (N-acetyl-5-methoxytryptamine), resulting in high blood levels at night and low levels during the daytime.[39,45] The daily, rhythmic melatonin signal contributes to the temporal coordination of normal behavioral and physiologic functions associated with the promotion of animal health and wellbeing.[7-10,12,19,25,54] Therefore, exposure to light in an intensity-, duration-, and wavelength- (spectral quality [that is, color]) dependent manner at a given time of day is essential to the regulation of the 'molecular clock' of the SCN.[2,3,7-12,32,49] Alterations in any of these parameters at a given time of day significantly influences endogenous circadian nighttime levels of melatonin in most mammals and may lead to various disease states, including metabolic syndrome,[27,28,43,44,48,51] obesity,[30,51,62,63] and carcinogenesis.[4-6,19,23,24] Studies from our laboratory have demonstrated that melatonin exerts regulatory effects on the uptake of linoleic acid (LA) and its metabolism to 13-hydroxyoctadecadienoic acid (13-HODE), glucose and lactate metabolism (Warburg effect), as well as several major neurohormones in humans and rats, and plays an integral role in tumor incidence, metabolism, and growth.[4-6,17-25,58]

Received: 01 Nov 2017. Revision requested: 18 Dec 2017. Accepted: 23 Jan 2018.
Departments of [1]Structural and Cellular Biology and [2]Comparative Medicine, Tulane University School of Medicine, Tulane, Louisiana
[*]Corresponding author. Email: rdauchy@tulane.edu

Recently, we showed that nude male rats maintained under daytime broad-spectrum (350 to 750 nm) cool white fluorescent (CWF) lighting filtered through blue-tinted cages had markedly elevated nighttime melatonin levels; this increased melatonin concentration extended into the early light phase and significantly inhibited tumor metabolism, signal transduction activity, and growth in PC3 human cancer xenografts.[24] We subsequently demonstrated that nighttime plasma melatonin levels in rodents maintained in daytime light-emitting-diode (LED) lighting that was enriched in the blue-appearing portion (465 to 485 nm) of the visible spectrum (bLAD) were 7-fold higher than those in rats maintained in broad-spectrum (CWF) lighting.[25] Furthermore, the melatonin duration extended 4 h into the light phase, presumably due to hyperproduction of melatonin during the night.

LED lighting is a rapidly emerging technology in vivaria and workplaces globally and offers many advantages over the incandescent or CWF lighting commonly in use today; these benefits include superior spectral control, energy efficiency, and overall long-term cost savings.[36,41] Little is known, however, regarding the long-term use of LED lighting and its potential effect on either behavior, physiology, and metabolism in humans and laboratory animals, and still less is known pertaining to cancer and metabolic diseases. In our previous study,[25] using new lighting measurement metrics to analyze our metabolic and physiologic findings,[38] we provided compelling evidence that animals exposed to bLAD compared with CWF lighting displayed a phenotype indicative of enhanced health and well-being.

More than 39,000 men and women in the United States alone this year will be diagnosed with liver cancer, with a 17.5% mortality rate within 5 y.[1] Incidence and mortality rates for liver cancer have risen markedly over the past several years, particularly in developing countries, such that liver cancer has become sixth most common cancer worldwide and second leading cause of death. Although the major risk factors are generally understood for certain cancers including lung, liver, and stomach,[1,37] other important environmental risk factors have come under scrutiny more recently.[60] Exposure to light at night, due to its ability to inhibit the nocturnal circadian pineal melatonin production, is associated with an increased risk of breast, prostate, and endometrial cancers reported in rotating night-shift workers.[26,34,46,59,61]

Both in vitro and in vivo studies have shown that melatonin inhibits the growth of a variety of human and animal tumors, including rodent hepatomas.[6,19] For their bioenergetic needs in supporting biomass formation, cancer cells depend primarily on aerobic glycolysis (Warburg effect) over oxidative phosphorylation.[5] The Warburg effect is characterized by increased tumor uptake of glucose and lactic acid production despite an overabundance of oxygen. Studies have shown those signal transduction pathways that include extracellular signal-regulated kinase p44/46 (ERK1/2) and signal transducer and activator of transcription 3 (STAT3) drive the Warburg effect.[4-6,14] In addition, tumor cells rely on the uptake of the ω6 fatty acid linoleic acid (LA), most prevalent in the western diet.[57] In most cancers, LA uptake occurs through a cAMP-dependent transport mechanism whereby LA is metabolized to the mitogenic agent 13-hydroxyoctadecadienoic acid (13-HODE).[58] In turn, 13-HODE enhances downstream phosphorylation of ERK1/2 activation of the Warburg effect, leading to enhanced tumor growth.

Melatonin inhibits processes of cancer initiation, progression, and growth in vivo.[5,55] The circadian nocturnal melatonin signal inhibits LA uptake and metabolism to 13-HODE, the Warburg effect in both human and rodent tumors, and actually drives circadian rhythms in tumor metabolism, signal transduction activity, and proliferation. These effects are extinguished when melatonin production is suppressed by light at night[5,16,18] and amplified when bLAD enhances melatonin production at daytime.[24]

The overall purpose of the present study was to compare the influence of daytime bLAD lighting, which is high in the emission of blue-appearing short wavelength light in the visible spectrum, with that of broad-spectrum CWF light on uptake and metabolism of linoleic acid, Warburg effect, signaling activity, and growth progression in rodent hepatoma 7288CTC in vivo. Specifically, we examined the hypothesis that, compared with those of standard CWF lighting, the spectral characteristics (color) of bLAD light not only amplifies the nighttime circadian melatonin signal but also alters the circadian regulation and enhances the suppression of metabolism, signaling activity, and growth of rodent 7288CTC hepatomas in male rats.

Materials and Methods

Reagents. HPLC-grade chloroform, ethyl ether, methanol, glacial acetic acid, heptane, hexane, and Sep-Pak C18 cartridges for HPLC extraction of samples were purchased from Fisher Chemical (Pittsburgh, PA). Free fatty acid (FFA), cholesterol ester, triglyceride, phospholipid, and rapeseed oil methyl ester standards as well as boron-trifluoride methanol, potassium chloride, sodium chloride, and perchloric and trichloroacetic acids were purchased from Sigma Scientific (St Louis, MO). The HPLC standards (±)5-HETE (catalog no. 34210) and 13(S)-HODE (catalog no. 38610) and ultrapure water (catalog no. 400000) were purchased from Cayman Chemical (Ann Arbor, MI).

Animals, housing conditions, and diet. The male, nonpigmented, inbred Buffalo rats (*Rattus norvegicus*; BUF/CrCrl; *n* = 15; age, 3 to 5 wk) used in this study were purchased from Charles River (Wilmington, MA). Animals were maintained in an AAALAC-accredited facility in accordance with the *Guide for the Care and Use of Laboratory Animals*.[40] All procedures for animal use were approved by the Tulane University IACUC.

Rats were maintained as described in autoclaved cages containing hardwood maple bedding (catalog no. 7090, Sanichips, Envigo Teklad, Madison, WI; 2 bedding changes weekly). To ensure that all rats remained infection-free from both bacterial and viral agents, serum samples from sentinel animals were tested quarterly and throughout this study by using Multiplex Fluorescent Immunoassay 2 (IDEXX Research Animal Diagnostic Laboratory, Columbia, MO), as described previously.[17,22-25,64] Throughout the experiment, dietary and water intake and body weight of rats were measured once daily, at 0800. Animals were given free access to diet (no. 5053 Irradiated Laboratory Rodent Diet, Purina, Richmond, IN) and acidified water. Quadruplicate determinations showed that 100 g of this diet contained 4.70 g total fatty acid (TFA), composed of 0.69% myristic (C14:0), 13.77% palmitic (C16:0), 1.18% palmitoleic (C16:1n7), 3.63% stearic (C18:0), 23.07% oleic (C18:1n9), 51.20% linoleic (C18:2n6), 6.13% γ-linolenic, and 0.25% arachidonic (C20:4n6) acids. Minor amounts of other FA comprised 0.09%. Conjugated LA and *trans* FA were not found. More than 90% of the TFA was in the form of triglycerides; more than 5% was in the form of FFA.

Caging, lighting regimens, and spectral transmittance measurements. After a 1-wk acclimation period under control lighting conditions (standard CWF lighting) rats were randomized into 2 designated groups of 6 control (CWF; 2 rats per cage) and 9 experimental (LED lighting; 3 cages of 2 rats, 1 cage of 3 rats) in standard translucent laboratory rodent cages (10.5 in. × 19 in. × 8 in.; wall thickness, 0.10 in.). Standard rodent cages used in this

study were purchased from Ancare (polycarbonate translucent clear, catalog no. R20PC, Bellmore, NY). The SPF animals were maintained in environmentally controlled rooms (25 °C; humidity, 50% to 55%) with diurnal lighting (12:12-h light:dark cycle; lights on, 0600). The CWF control animal room was lighted with a series of 2 overhead luminaires containing 4 standard soft, cool-white (2700 lm; 4100 correlated-color temperature) fluorescent lamps per ballast (F32T8TL841, model 272484, Alto II Collection, 32 W, 48 in., Series 800, Philips, Somerset, NJ). The experimental LED animal room was lighted with a series of 2 overhead luminaires containing 4 LED lamps, high in emission of blue-appearing portion of the visible spectrum (465 to 485 nm; 2650 lm > 5000 color-corrected temperature) lamps per ballast (12T8/AMB/48 [model 9290011242], T8 12 W, 48 in., Philips). Animal rooms were completely devoid of light contamination during the dark phase.[18,19]

Lighting, lighting regimens, and spectral transmittance measurements have been described in detail previously.[25] Briefly, daily throughout the experiment, normal light-phase lighting intensity was measured at 1 m above the floor in the center of the room (at rodent eye level) and outside and from within and at the front of the animal cages. Irradiance measures were recorded by using a radiometer–photometer (model no. IL-1400A, International Light Technologies, Peabody, MA) with a silicon diode detector head (model no. SEL033), which included a wide-angle input optic (W6849) and filter (F23104) that provided a flat response across the visible spectrum. Illuminance measures used a silicon diode detector head (model no. SEL033), which included with a wide-angle input optic (W10069) and filter (Y23104) to provide a photopic illuminance response. The meter and associated optics were calibrated annually, as described previously.[17-19,22-25]

At the same time daily (0800), prior to light intensity measurements, all cages on the rack were rotated one position to the right (at a premeasured identical distance apart) in the same horizontal plane. There were no significant differences in light intensity, as measured outside and from within the front of each cage at the different positions. The daily cage shift, however, ensured uniformity of intensity of ocular light exposure by the animals and accounted for the effects of any unforeseen subtle differences due to the position on the rack. As described previously,[25] measures of lux, appropriate for daytime vision assessment, are reported with radiometric values of irradiance (μW/cm^2), as appropriate for quantifying light stimuli that regulate circadian, neuroendocrine, or neurobehavioral physiology in animals and humans.

Spectral power measurements. The spectral power of the respective CWF and bLAD light sources in this study were measured by using a handheld spectroradiometer (FieldSpec, Analytic Spectral Devices [ASD], Boulder, CO) with a cosine receptor attachment as described in detail previously.[25] Spectral power distributions, a measure of the concentration (as a function of wavelength) of any radiometric quantity (that is, irradiance compared with wavelength), were recorded at a distance of 30 cm, with the meter pointing directly at the light source for 1 s.

Calculation of effective rod, cone, and melanopsin photoreceptor illuminances. Calculation of the effective rodent rod, cone, and melanopsin photoreceptor illuminances for this species and strain, has been previously reported.[25] Briefly, spectral power distributions for the experiments shown here were entered into a ToolBox worksheet, which is a software model for rodent photoreception that is freely available online.[52] The spectral power distribution measurements for the experiments were imported into the worksheet in 1-nm increments between 325 and 782 nm. ToolBox lists the rodent spectral range as extending to 298 nm, beyond the range of the spectroradiometer we used in this study. As directed in the ToolBox instructions, values between 298 nm and 325 nm were manually changed to 0.

Arterial blood collection. After 2-wk exposure to the lighting regimens, arterial blood collection for melatonin analysis was made as described previously.[4-6,16-19,22-25] Briefly, rats underwent a series of 6 low-volume blood draws by cardiocentesis to collect left ventricular-arterial blood over a period of 30 d (total blood collected equaled 1.2 mL/animal). Blood collections (0.1% volume/body weight each sample; 0.2 mL) in this IACUC-approved protocol, were designated at 4-h intervals to include the 24-h feeding period; each animal was tested only once every 5 d to eliminate the effects on feeding, stress, and potential mortality.

Melatonin analysis. Arterial plasma melatonin levels were measured by radioimmunoassays using a rat ^{125}I radioimmunoassay kit (catalog no. 01-RK-MEL2; lot no. 2535.5.U; Bühlmann Laboratories, Schönenbuch, Switzerland) and analyzed by using an automated gamma counter (Cobra 5005, Packard, Palo Alto, CA) as previously described.[22-25,64] The minimal detection level for the assay was 1 to 2 pg per milliliter of plasma.

Tumor implantation and growth. At 1 wk after final blood collection for melatonin analysis, after a total of 41 d of exposure in either the CWF or bLAD lighting environments, all rats were implanted with tissue-isolated Morris 7288CTC hepatomas as described previously.[20,21,56] Briefly, animals anesthetized by using ketamine (80 to 100 mg/kg IP)–xylazine (5 to 10 mg/kg IP) solution (MWI Veterinary Supply, Meridian, IN) delivered through a 25-gauge, 5/8-in tuberculin syringe (Becton Dickenson, Franklin Lakes, NJ) were placed supine on the preparation surface, and the skin in the lower left quadrant was removed by using an electric shaver. The shaved area was cleansed with isopropyl alcohol, treated with povidone–iodine solution, rinsed with warm sterile water, and allowed to dry. Rats received buprenorphine (0.05–0.1 mg/kg SC 2 or 3 times daily; MWI Veterinary Supply) through a tuberculin syringe just prior to surgery to minimize discomfort, distress, and pain. A 3-mm cube of tumor was attached (by using a single suture of 5-0 black braided silk; Ethicon, Cincinnati, OH) to the end of a vascular stalk composed of the truncated left superficial inferior epigastric artery and vein of the rat. The tumor implant and vascular stalk were enclosed in a small sterile parafilm envelope, placed back in the inguinal fossa, and the skin incision was closed with 4-0 Polysorb braided absorbable suture (Covidien, Mansfield, MA). In addition, ophthalmic lubricant was applied to the rats' eyes to prevent eye irritation and corneal drying.

The rodent hepatomas grew subcutaneously as tissue-isolated implants in the left inguinal fossa. Arterial blood supply to and venous drainage from the implant are established through the epigastric vessels; the paraffin envelope blocks vascular connections to other host tissues. Tissue-isolated tumors typically do not develop large areas of central necrosis as do subcutaneous tumors that receive their blood supply from the periphery. Latency-to-onset of tumor mass (that is, from the first day of implantation to first palpable, pea-size mass) and growth rates (g per d) were generated by linear regression analysis during the study; final, actual tumor weights were determined by weighing at the end of the experiment.[4,19,20,56] Briefly, tumors were measured by using calipers (model no. 1464817, Fisher Scientific, Waltham, MA) for length, width, and depth and converted to cm^3. This value was inserted into the linear regression formula $y = mx + b$, where y (in grams) is [0.59 × (tumor volume in cm^3)] + 0.79 g, as used for measurement in our laboratory for nearly

40 y.[20] The tumor estimated weight is compared with the actual final weight and has now had a comparative accuracy of greater than 99%, or within 0.1 g. Nonetheless, for purposes of this study, we used the final, actual tumor weights for calculation of tumor arteriovenous (A–V) difference comparisons.

To determine the effects of normal daytime physiologic (less than 10 pg/mL; occurring at 1200) and elevated nighttime (occurring at 2400) melatonin levels on tumor A–V differences in rats maintained in either CWF or bLAD lighting environments, all rats were randomized into 5 designated groups of 3 animals per cage: group I, 0800 harvest; group II CWF, 2400 harvest; group III bLAD, 0800 harvest; group IV bLAD, 1200 harvest; and group V bLAD, 2400 harvest. Animal cages were rotated as described earlier.[25]

Tumor arteriovenous difference measurements. When tumors reached 5 to 7 g in estimated weight, a point of equivalence as a common milestone, animals were prepared for A–V assessments in vivo between 0600 and 0800.[4,16,19-21,56] Procedures for anesthesia and heparinization for the tumor-bearing animals, the surgical preparation of the tumor, and technical procedures for collection of blood from the tissue-isolated tumors in situ have been described previously.[25,56] Briefly, rats were anesthetized with ketamine (80 to 100 mg/kg IP)–xylazine (5 to 10 mg/kg IP), whole blood was collected, and pH, pO_2, pCO_2, glucose, and lactic acid levels were measured (iSTAT1 Analyzer, Abaxis, Union City, CA; $G4^+$ and $G8^+$ cartridges, Abbott Laboratories, East Windsor, NJ). Values for glucose and lactate are reported as mg/dL and mmol/L and for pO_2 and pCO_2 as mm Hg, respectively. Minimal detection levels for pH, pO_2, pCO_2, glucose, and lactate were 0.01, 0.1 mm Hg, 0.1 mm Hg, 0.2 mg/dL, and 0.01 mmol/L, respectively. Plasma samples were obtained for analysis of Hct, TFA and LA uptake, and 13-HODE production. At the end of the tumor A–V measurements (bLAD groups III through V, day 39 after implantation; CWF control groups I and II, day 19 after implantation), rats were exsanguinated by using carotid catheters, tumors were freeze-clamped under liquid nitrogen, weighed, and stored at –80 °C until used for analysis.

FA extraction and analysis, tumor 13-HODE production, and determination of tumor cAMP levels. Arterial plasma and tissue TFAs were extracted from 0.1 mL arterial and venous samples following the addition of heptadecanoic acid (C17:0), methylated and analyzed via gas chromatography as previously described.[4-6,-23,59] Tissue TFA and LA levels in control and experimental groups were extracted from 0.1mL of blood plasma or 0.2 mL of 20% homogenates, as previously described.[15-25,56-58] Tumor TFA and lipid fractions (that is, triglycerides, phospholipid, FFA, and cholesterol esters) were separated by using silica gel G plates (catalog no. 01011, Uniplate, Alltech, Newark, DE), as described previously.[16,24,57,58] Methyl esters of FA were analyzed by using a gas chromatograph (model no. HP 5890A, Hewlett-Packard, Palo Alto, CA) equipped with a fused-silica capillary column (30 × 0.25 mm [inner diameter]; film thickness, 0.25 µm; catalog no. 2330, Supelco, Bellefonte, PA). Values for FA represent the sum of the 7 major fatty acids (myristic, palmitic, palmitoleic, stearic, oleic, linoleic, and arachidonic acids) present in tumor tissue as FFA, cholesterol esters, triglycerides, and phospholipids, as well as other tumor lipids. The minimal detectable limit for the assay was 0.05 µg/mL. For statistical comparisons, rates of tumor TFA and LA uptake are presented as both absolute values and as percentages of supply.

HPLC analysis of 13-HODE production. Tumor production of 13-HODE was measured as previously described, by using 0.2-mL arterial and venous plasma samples[24,58] collected in vivo and combined with a known internal standard (racemic 5-hydroxy, 6,8,11,14-eicosatetraenoic acid, Cayman Chemicals). All13-HODE production values by 7288CTC hepatomas are expressed as nanograms per minute per grams of tumor. Values of 0 indicated that no 13-HODE was detected within the sensitivity range of the instrument (10^{-18} M and higher).

Determination of tumor cAMP, DNA content, and [^{3}H]thymidine incorporation into DNA. Tumor levels of cAMP were determined by using ELISA (GE Lifesciences, Piscataway, NJ), and [^{3}H]thymidine incorporation into DNA and DNA content was determined as described previously.[21,23,24]

Western blot measurement of tumor phosphorylated kinases. Frozen tumor tissue was pulverized to a fine powder under liquid nitrogen, weighed, and lysed in Tissue Extraction Reagent I (catalog no. FN0071, Invitrogen, Camarillo, CA) containing Tris (50 mM, pH 7.4), EDTA (20 mM), NP40 (0.5%), NaCl (150 mM), PMSF (0.3 mM), NaF (1 mM), $NaVO_4$ (1 MM), dithiothreitol (1 mM), and protease and phosphatase inhibitor cocktails (protein:inhibitor, 100:1 [v/v]) and homogenized by using a Potter–Elvehjem homogenizer (Wheaton Science Products, Millville, NJ). The tissue lysates were centrifuged for 10 min at 10,000 × *g*, 4 °C. Protein concentrations of the supernatants were determined by using a kit (Bio-Rad, Hercules, CA). Total protein (90 µg per sample) was separated electrophoretically on a precast gel (Criterion, Bio-Rad, Richmond, CA) and transferred onto nitrocellulose membranes (Bio-Rad). After incubation with 5% nonfat milk in Tris-buffered saline containing 0.05% Tween, the immunoblots were probed with various antibodies including extracellular signal-regulated kinase (phosphorylated ERK1/2 Thr202/Tyr204, total ERK1/2; and phosphorylated STAT3 [Tyr707] and total STAT3; Cell Signaling ,Danvers, MA). The blots were stripped and reprobed with antiβ-actin antibody (Sigma) to evaluate loading. Quantitation of Western blots and differences in expression of total and phosphorylated proteins were determined by digital quantitation of phosphorylated and total protein levels (Infrared Imaging System and software; Licor Biosciences, Lincoln, NE), by normalizing phosphorylated levels to the levels of the total protein of interest and comparing the levels of group I (0800) compared with group II (2400); group I compared with group III (0800); group I compared with group IV (1200); group I compared with group V (2400); group II (2400) compared with group III (0800); group II compared with group IV (1200); group II compared with group V; group III compared with group IV; group III compared with group V; and group IV compared with group V to determine the percentage or fold change.

Statistical analysis. Unless otherwise noted, all data are presented as the mean ± 1 SD of 6 animals for CWF control group and 9 animals for the LED experimental group. Statistical differences among group means in the tumor A–V measurement studies were determined by one-way ANOVA followed by the Bonferroni multiple-comparison test. Differences in slopes of regression lines (that is, tumor growth rates) among groups were determined by regression analysis and tests for parallelism (Student *t* test). Differences were considered to be statistically significant at a *P* value of less than 0.05. Student *t* test, one-way ANOVA followed by Bonferroni posthoc testing, and linear regression analyses were all performed by using Prism 5 (GraphPad Software, La Jolla, CA).

Results

Animal-room illumination. Animal-room illumination during the daytime at the center of each room and at 1 m above the floor (with the detector facing upward toward the luminaires) varied minimally during this study (*n* = 120 measurements).

Illuminance and irradiance values were 498.3 ± 12.23 lx (203.83 ± 5.03 µW/cm²) in the control CWF room and 499.46 ± 13.49 lx (205.20 ± 5.55 µW/cm²) in the experimental LED room. Measurements of photometric illuminance (lx) and radiometric irradiance (µW/cm²) within the cages of each group are a result of a mean of the values taken at 6 locations within the cages with the detector facing forward (front, center, and rear on right and left sides of cage) at all cage positions to accurately account for actual ocular light levels within the cages independent of the animal location. Average interior ocular light levels showed little to no intercage or intergroup variability (n = 648 measurements) and are reported here for the CWF and LED groups, respectively, at 156.80 ± 4.72 lx (64.13 ± 1.93 µW/cm²) and 159.39 ± 6.80 lx (65.19 ± 2.78 µW/cm²). Normalized spectral power distributions of the CWF and LED lights used in this study were reported previously.[25] The fluorescent lamp yielded signature peaks in the appropriate wavelengths (545 and 612 nm) for this type of light. The LED lamp showed a standard blue LED-enhanced phosphor spectral power distribution, with a peak at 448 nm. In terms of total energy in the 465-to-485–nm range, the LED lamp had more than 50% higher photic emissions than compared with the CWF lamp. Calculated photon flux, irradiances, and weighted rodent photopigment illuminances for both lights used in the study have been published previously.[25] The data illustrate that, although photon flux and irradiance are similar in the 2 lights, they yield marked differences (P < 0.05) in terms of stimulation of the rodent photoreceptors. As demonstrated, regarding potential light stimulation of the melanopsin-containing ipRGC, the LED lamp was calculated to have more than 30% higher photic emission stimulation capability compared with the CWF lamp.[25]

Animal food and water intakes and growth measurements. Food and water intakes and body growth rates differed significantly (P < 0.05) between the tumor-bearing rats maintained in the CWF compared with LED lighting regimen during this study. Mean (n = 42 measurements) daily dietary intake for animals in CWF and LED groups, respectively, were 13.38 ± 0.16 g per 100 g body weight daily and 12.72 ± 0.30 g per 100 g body weight daily, representing a 5.2% ± 0.1% increase in average daily dietary intake of CWF over LED rats. Water intake was 15.04 ± 0.08 mL per 100 g body weight daily and 13.73 ± 0.12 mL per 100 g body weight daily for the CWF and LED groups, respectively, representing an 8.7% ± 0.02% increase in average daily water intake for CWF over LED animals. The mean (n = 42 measurements per group) body growth rates for CWF and LED groups were 4.28 ± 0.32 g/d and 3.39 ± 0.51 g/d.

Plasma melatonin levels. Circadian rhythms in concentrations of plasma melatonin for animals maintained under CWF and bLAD lighting conditions are depicted in Figure 1. Although the overall pattern of daily melatonin level rhythms was the same for both groups, peak height and phase duration differed markedly. Melatonin levels in the bLAD group began to rise rapidly after the onset of the dark phase, reaching the peak of those of the CWF group (control) by 2000. The peak level for bLAD animals (group V, 2400) was more than 7-fold higher (P < 0.001) than that of the controls (group II) at the same point. Arterial plasma melatonin levels remained more than 3-fold higher in the bLAD compared with CWF group even at 4 h after the onset of the light phase, finally reaching normal daytime levels (less than 10 pg/mL) at 1200. The integrated mean levels of melatonin over the 24-h period for bLAD rats (1651.0 pg/mL) were more than 7-fold higher than those of rats maintained under CWF lighting (224.5 pg/mL).

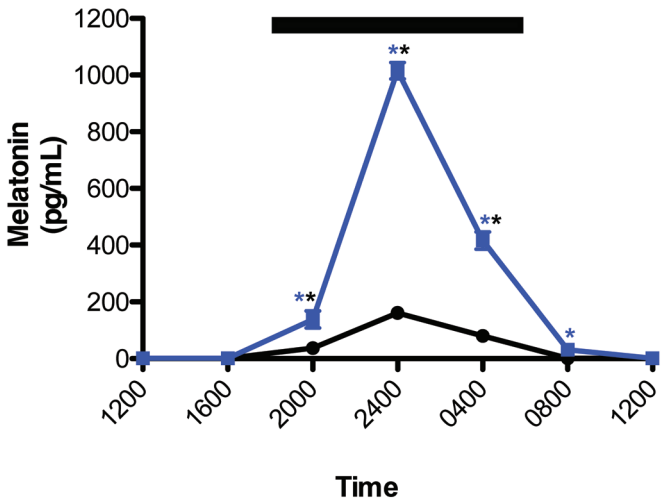

Figure 1. Circadian plasma melatonin levels (pg/mL; mean ± 1 SD) of nonpigmented male Buffalo rats maintained for 2 wk in standard polycarbonate, translucent, clear cages in cool-white fluorescent (CWF; controls, solid black circles; n = 6) or blue-light–enriched (bLAD; experimental, solid blue squares; n = 9) lighting under a LD,12:12-h photoperiod prior to tumor implantation. Both groups were exposed similarly during the light phase (300 lx; 123 µW/cm²); during the 12-h dark phase (1800 to 0600, dark bars), animals were exposed to no light at night. Concentrations with asterisks differ (P < 0.05) from concentrations without asterisks.

Tumor growth rates. The latency-to-onset of tumor appearance after hepatoma implantation, measured as the time between implantation until first palpable mass (approximately 10 mm³), and the tumor growth rate were 11 d and 0.71 ± 0.03 g/day in CWF groups (I and II) and 21 d and 0.36 ± 0.03 g/day in bLAD groups (III through V), respectively (Figure 2). These values represent a nearly 50% increase (P < 0.05) in latency-to-onset and a 50% decrease in tumor growth rates in rats maintained in bLAD compared with CWF lighting. Although the mean tumor weight was nearly identical between the groups at time of harvest (CWF groups [I and II], 7.03 ± 0.31 g; bLAD groups [III–V], 7.05 ± 0.30 g), the day of tumor harvest was delayed by more than 100% in rats in bLAD (day 39 after implantation; when tumors became comparable in size with those of CWF groups I and II) compared with CWF lighting (day 19).

Tumor A–V measurements. We assessed whether tissue-isolated hepatomas themselves exhibited differences in cAMP levels, TFA and LA uptake, 13-HODE release, [³H]thymidine incorporation into tumor DNA, DNA content, and Warburg effect as a result of daytime bLAD exposure and altered arterial plasma melatonin levels at the time of harvest (Table 1). None of the tumor levels of these constituents in group I (0800) were different from those of group IV (1200) when arterial plasma melatonin levels were at normal physiologic daytime concentrations (less than 10 pg/mL). Tumor cAMP levels, TFA and LA uptake, [³H]thymidine incorporation into tumor DNA, DNA content, at 2400 were decreased significantly (P < 0.001) by 97.3%, 100%, 100%, 100%, 64.1%, and 29.8%, respectively, in CWF rats in group II compared with group I when normal nighttime melatonin levels were 98.6% higher than normal daytime levels. Tumor cAMP levels, TFA and LA uptake, [³H]thymidine incorporation into tumor DNA, and DNA content at 0800 were decreased significantly (P < 0.001) by 83.4%, 76.7%, 77.9%, 81.6%, 53.1%, and 23.4%, respectively, in rats in bLAD group III compared with CWF group I. These same parameters were still markedly depressed (P < 0.001) by 78.0%, 64.1%, 66.0%, 79.2%,

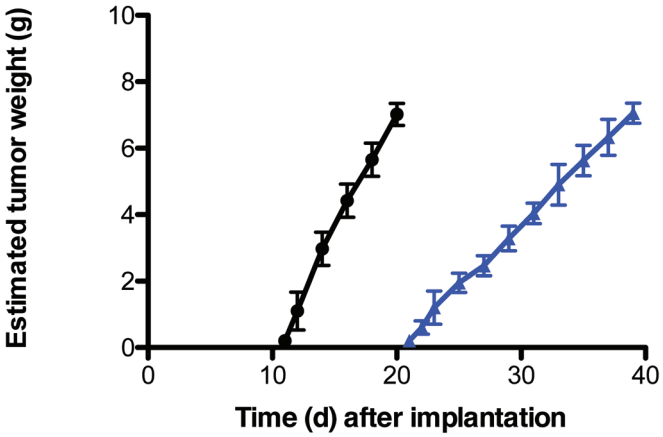

Figure 2. Effects on tissue-isolated 7288CTC hepatomas in male Buffalo rats after implantation (day 0) in animals exposed to bLAD at daytime (solid blue triangles) compared with those exposed to CWF light (solid black circles). Each point represents the estimated tumor weight (mean ± 1 SD); $n = 10$, bLAD; $n = 6$, CWF). Tumor growth rates differed significantly ($P < 0.001$) between groups.

47.9%, 18.2%, respectively, in bLAD group III (0800) compared with bLAD group IV (1200), when melatonin levels remained more than 150% higher than the normal daytime (0800) levels in CWF group I (2.17 pg/mL). Tumor cAMP levels, TFA and LA uptake, 13-HODE release, [^{3}H]thymidine incorporation into tumor DNA, and DNA content were depressed by 96.5%, 100%, 100%, 100%, 68.7%, 29.5%, respectively, in bLAD group V (2400), when melatonin levels were nearly 4120% higher, compared with bLAD group IV (1200).

Arterial glucose supply to the tumors and A–V differences for glucose, lactate, pO_2, and pCO_2 in vivo were measured across the implanted hepatomas of the CWF and bLAD groups at 0800, 1200, and 2400 (Table 2; Figure 3). The rates of tumor glucose uptake and lactate production and of O_2 uptake and CO_2 release in CWF group II (2400) were decreased significantly ($P < 0.001$) by 65.9%, 53.3%, 29.7%, 35.4%, respectively, compared with those parameters of CWF group I (0800). The rates of tumor glucose uptake and lactate production and of O_2 uptake and CO_2 release in bLAD group III (0800) were decreased ($P < 0.001$) by 41.2%, 28.9%, 18.4%, and 34.6%, respectively, compared with CWF group I (0800). These same parameters were still markedly depressed ($P < 0.001$) by 37.8%, 22.3%, 19.2%, and 24.8%, respectively, in bLAD group III (0800) compared with bLAD group IV (1200), when melatonin levels remained more than 150% higher than the normal daytime (0800) levels in CWF group I (2.17 pg/mL). The rates of tumor glucose uptake and lactate production and of O_2 uptake and CO_2 release were depressed by 73.2%, 59.3%, 40.4%, and 41.1%, respectively, in bLAD group V (2400) compared with bLAD group IV (1200) and were depressed an additional ($P < 0.05$) 36.7%, 24.0%, and 17.6%, respectively, in bLAD group V (2400) compared with group II (2400), when nighttime circadian melatonin levels were elevated so dramatically above normal physiologic levels.

Within each tumor group ($n = 3$/group; groups I through V), whole-blood acid-gas analysis, arterial and venous pH, O_2 saturation, Hct, and tumor venous blood flow fluctuated by less than 1% throughout blood collection and are reported here as the mean ± 1 SD of combined values for both CWF and bLAD animals. Arterial and venous pH were, respectively, 7.45 ± 0.03 and 7.31 ± 0.02. Arterial O_2 saturation remained constant throughout the hepatoma venous blood collections (99.3% ± 0.2%). Arterial and venous Hct were 43.6% ± 1.9% and 46.5% ± 1.8%, respectively, representing approximately 6% hemoconcentration of the blood as it passed through the tumor. Tumor venous blood flow was 0.129 ± 0.002 mL/min. Because of these effects, the tumors were considered to be in steady-state when 15 min passed with less than a 5% change in blood flow or when a reversible change had minimal effects on nutrient uptake or release.

FA content of 7288CTC hepatomas. The TFA contents and lipid fractions (mean ± 1 SD) of the 7288CTC hepatomas excised from animals maintained in either CWF (groups I and II) or bLAD (groups III through V) lighting conditions were measured in rats with free access to food (Table 2). The total FA content of groups I and II was 1.8 times higher than for groups III through V. FA composition for CWF and bLAD groups revealed a similar trend, insofar as triglycerides, phospholipids, FFA, and cholesterol esters are concerned. As shown (Table 2), levels of the 7 major fatty acids comprising the TFA content were significantly ($P < 0.05$) higher in tumors of animals maintained in CWF compared with bLAD lighting. LA (C18:2), the principal growth-stimulatory FA, was in greatest abundance (CWF, 40.4% ± 0.6%; bLAD, 40.0% ± 0.5%), followed by palmitic (C16:0) and oleic (C18:1) acids, and corresponding well with the proportional increase in the arterial blood plasma.[25] Indeed, individual FA examined on the basis of percentage of TFA showed a similar proportional increases. In terms of the sum total of lipid fractions for both CWF and bLAD, triglycerides were more abundant than phospholipids, followed by FFA and then cholesterol esters. However, triglycerides, phospholipids, FFA, and cholesterol esters were lower in bLAD compared with CWF groups by 21.5%, 78.8%, 89.2%, and 91.7%, respectively, with an overall suppression of total LA content of 43.1%.

Western blot analysis of ERK and STAT3. We next examined a potential signaling mechanism by which bLAD influences circadian system regulation of hepatoma LA uptake and metabolism, Warburg effect, signaling, and growth. We focused on the oncogenic metabolic signaling pathways of ERK and STAT3, both of which are important transcriptional regulators of the Warburg effect.[5,33] Figure 4 shows downregulation of phosphorylated ERK1/2 in hepatomas harvested at nighttime (2400), when melatonin levels are high for both the CWF and bLAD groups, and upregulation during the light phase (1200), when the melatonin signal is low. Enhanced downregulation of the ERK1/2 signaling pathway was further revealed in bLAD group V (2400) compared with bLAD group IV (2400), when the nighttime circadian melatonin signal was more than 7-fold higher. Interestingly, compared with both CWF group I and bLAD group III (0800 and 1200), hepatomas of CWF group II (0800) demonstrated significant downregulation of this signaling pathway, corresponding to the higher plasma melatonin levels in CWF group II (0800) that extended into the daytime from the elevated nighttime levels of bLAD group V (2400). STAT3, which has been shown to be constitutively phosphoactivated in most tumors,[33] was unaffected by any of the light exposure regimens and thus was upregulated in all groups of 7288CTC hepatomas.

Discussion

The present findings support the presence of a dynamic, circadian interaction between LA metabolism in hepatomas and the Warburg effect (that is, glucose uptake and lactate production); this interaction was aligned and in balance with circadian-driven host factors under light–dark-entrained conditions, which were modulated by exposure to bLAD compared with CWF daytime lighting conditions. Intensity, duration, and

Table 1. Effects of daytime (0800 h and 1200 h) and nighttime (2400 h) arterial blood plasma melatonin concentration in hepatoma 7288CTC tumor xenografts in situ in groups I and II (controls) and III through V (bLAD)

Group	cAMP (nmol/g tissue)	Total fatty acid uptake (μg/min/g)	LA uptake (μg/min/g; [%])	13-HODE (ng/min/g)		[^{3}H]-thymidine incorporation (dpm/μg DNA)	DNA content (mg/g)	Plasma melatonin (pg/mL)
				Arterial supply	Venous output			
I (0800)	1.178 ± 0.114	11.74 1.66 (46.0 ± 2.6%)[a]	4.02 + 0.41 (46.6 ± 3.1%)[a]	ND	42.61 ± 1.29	50.7 + 2.5	4.7 + 0.2	2.17 ± 1.10
II (2400)	0.032 ± 0.007[b]	−0.07 ± 0.06[d] (−0.2 ± 0.1%)[a]	0.03 ± 0.03[b] (−0.2 ± 0.2%)[a]	ND	ND[b]	18.2 + 1.1[b]	3.3 + 0.2[b]	152.5 ± 16.6[b]
III (0800)	0.195 ± 0.077[b,c]	2.73 + 0.57[d,e] (12.0 ± 2.5%)[a]	0.89 ± 0.18[b,c] (11.2 ± 2.9%)[a]	ND	7.82 ± 2.42[b,c]	23.8 + 2.0[b,c]	3.6 + 0.1[b,c]	32.57 ± 4.83[b,c]
IV (1200)	0.889 ± 0.049[b,c,d]	7.60 ± 0.38[b,c,d] (43.0 ± 1.2%)[a]	2.62 ± 0.11[b,c,d] (43.9 ± 1.9%)[a]	ND	37.51 ± 2.87[b]	45.7 + 0.3[c,d,e]	4.4 + 0.3[b,d]	2.46 ± 0.89[b,d,e]
V (2400)	0.031 ± 0.008[b,d,e]	−0.04 ± 0.04[b,d,e] (0.1 ± 0.1%)[a]	−0.02 ± 0.02[b,d,e] (−0.1 ± 0.1%)[a]	ND	ND[b,d,e]	14.3. + 1.8[b,d,e]	3.1 + 0.1[b,d,e]	1016.1 ± 50.69[b,d,e]

ND, not detectable.
Data are given as mean ± 1 SD (n = 3/group). Tumor weight, 7.04 + 0.30 g (n = 15).
[a]Percentage of arterial supply.
[b]$P < 0.05$ versusgroup I (0800).
[c]$P < 0.05$ compared with group II (2400).
[d]$P < 0.05$ compared with group III (0800).
[e]$P < 0.05$ compared with group IV (1200).

wavelength of light at a given time of day entrains the SCN, by means of the circadian melatonin signal, which is essential in the regulation of circadian rhythms associated with animal metabolism and physiology.[7-12] As reported earlier, melatonin exerts regulatory effects on tumor LA uptake and metabolism to 13-HODE, glucose and lactate metabolism, as well as several major systemic hormones in humans and rats; in addition, melatonin plays an integral role in tumor incidence, metabolism, and growth.[4-6,17-25,58] Arguably, the marked circadian changes in signal to further suppress the Warburg effect, LA metabolism, signaling, and hepatoma growth in tumor-bearing rats. We used LED luminaires with 30% greater emissions for stimulating melanopsin-containing ipRGC and compared these with standard fluorescent luminaires used in laboratory animal housing facilities. The standard CWF and LED lamps we used in this study are some of the most commonly used lights in current laboratory animal science and biomedical research fields.[36,41,49] This study is the first to show that long-term exposure of rats

Table 2. Fatty acid composition and lipid content (μg/g tumor tissue) of hepatoma 7288CTC in 7288CTC tumor xenografts in situ in groups I and II (controls) and III through V (bLAD)

Fatty acid	12:12-h CWF (n = 6)					12:12-h bLAD (n = 9)				
	Triglycerides	Phospholipids	FFA	Cholesterol esters	Total	Triglycerides	Phospholipids	FFA	Cholesterol esters	Total
C14:0	121 ± 13	156 ± 70	7 ± 1	4 ± 3	309 ± 16[a]	128 ± 14	3 ± 2	3 ± 2	3 ± 2	136 ± 15
C16:0	2031 ± 125	1229 ± 273	129 ± 19	144 ± 30	3532 ± 380[a]	1714 ± 123	194 ± 29	14 ± 4	16 ± 4	1941 ± 119
C16:1	417 ± 19	512 ± 73	21 ± 8	27 ± 11	976 ± 90[a]	332 ± 50	34 ± 9	3 ± 2	4 ± 1	374 ± 54
C18:0	388 ± 28	256 ± 40	217 ± 77	78 ± 17	935 ± 120[a]	543 ± 99	150 ± 17	51 ± 15	3 ± 2	727 ± 120
C18:1	1279 ± 205	1141 ± 138	136 ± 25	82 ± 10	2633 ± 199[a]	1622 ± 68	98 ± 23	25 ± 9	5 ± 3	1751 ± 75
C18:2	4074 ± 416	1653 ± 413	416 ± 67	226 ± 22	6535 ± 503[a]	3496 ± 351	186 ± 48	11 ± 3	5 ± 2	3719 ± 350
C20:4	36 ± 2	250 ± 38	154 ± 37	69 ± 12	473 ± 37[a]	17 ± 2	183 ± 79	9 ± 4	16 ± 4	613 ± 61
Total	9309 ± 490	5228 ± 561	1072 ± 133	627 ± 60	16180 ± 886[a]	7010 ± 739	1109 ± 116	116 ± 32	52 ± 46	9294 ± 702

FFA, free fatty acids
Data are given as mean ± 1 SD (n = 6 for combined groups I and II; n = 9 for combined groups III through V).
[a]$P < 0.05$ compared with 12:12-h bLAD.

melatonin levels in animals exposed to bLAD may have been responsible for some of the circadian changes in these hormones that were observed in the previous and current studies in male and female rats.[25] We previously reported that male rats exposed to bLAD, compared with animals housed under CWF lighting, had a dramatically amplified nocturnal circadian melatonin signal, which altered markedly the circadian patterns of plasma measures of physiology and metabolism in normal and neoplastic tissues.[24,25] In light of these observations, we tested the hypothesis that exposure to bLAD—compared with CWF light—during the light phase amplifies the nighttime melatonin to daytime blue-enriched LED lighting induces amplification and prolongation of the nocturnal circadian melatonin signal, resulting in increased downregulation of hepatoma cAMP levels, LA uptake, 13-HODE production, the Warburg effect, signal transduction pathways (cAMP and ERK1/2) and substantially slower (more than 50%) tumor growth rates compared with those of hepatomas in rats exposed to the 'normal' nighttime physiologic melatonin signal generated under CWF lighting. The lack of an effect of different light exposures, and thus melatonin levels, on STAT3 expression is consistent with the

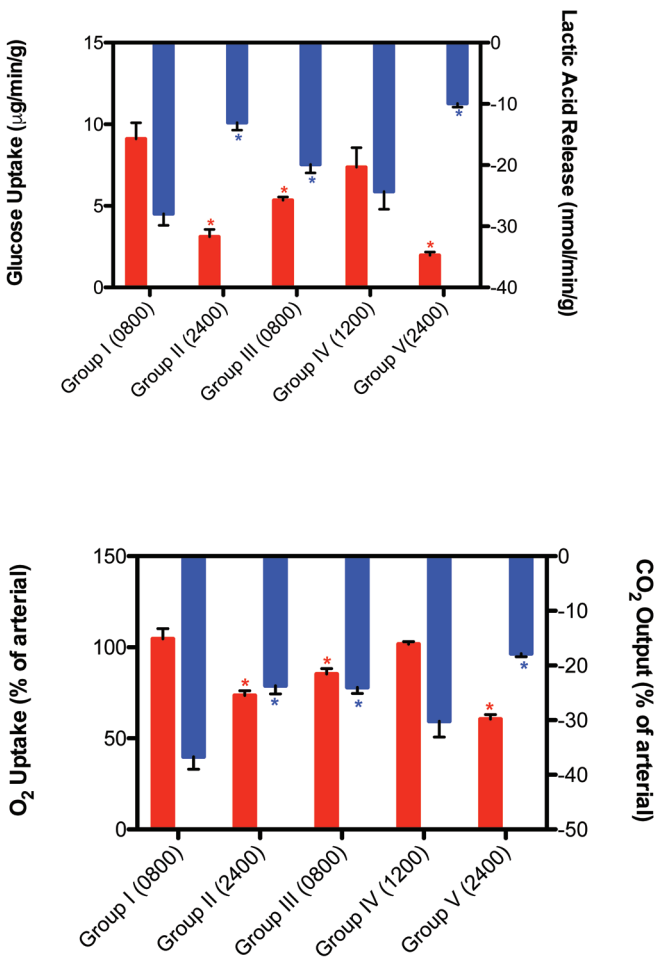

Figure 3. Effects on arterial–venous blood differences in glucose uptake (upper panel, red bars), lactate production (upper panel, blue bars), pO_2 uptake (lower panel, red bars), and pCO_2 production (lower panel, blue bars) in tissue-isolated 7288CTC hepatomas in male Buffalo rats in groups I through V under the 2 lighting conditions at the respective time of day. Concentrations with asterisks differ ($P < 0.05$) from concentrations without asterisks.

previously reported constitutive expression and phosphoactivation of STAT3 in hepatomas.[14]

This unusual phenomenon of bLAD-induced enhancement of the nocturnal melatonin signal was first observed in rats in our earlier investigation.[25] The underlying mechanism by which light wavelength induced this 7-fold increase in the nighttime circadian melatonin response over normal nocturnal levels is not yet clear. As demonstrated here and previously, the high-amplitude nighttime melatonin signal, in effect, extended 'biologic' night well into the light phase. The elevated nocturnal levels of circulating melatonin in the bLAD groups may be the result of hyperstimulation of pineal melatonin production due to hyperactivation of the rate-limiting enzyme, arylalkylamine-N-transferase, in the melatonin synthetic pathway.[42,45] A concomitant role of altered hepatic melatonin metabolism and its pharmacokinetics, may be an additional contributing factor. Interestingly, light has a gating effect on melatonin synthesis, whereby melatonin levels would normally plummet in response to the onset of the light phase (that is, 0600) if the extended melatonin duration was due strictly to continuing—albeit decreasing—pineal melatonin production. Nonetheless, we showed in naïve, nontumor-bearing rats that the circadian rhythms of all physiologic and metabolic analytes in the bLAD animals were altered in response to the different spectral characteristics of the blue-enriched LED light compared with broad-spectrum CWF light during the light phase. These alterations in rhythm amplitude, phasing, and duration appeared to be independent of general SCN activity, given that the circadian rhythm in food intake was preserved.

Results of previous tumor growth studies revealed that 7288CTC hepatomas are extremely sensitive to alterations in plasma melatonin levels in rats.[6,19] Physiologic nocturnal levels of this neurohormone have a marked oncostatic effect on hepatoma cAMP levels, activation of the ERK1/2 signal transduction pathway, LA and TFA uptake, 13-HODE production, the Warburg effect, and tumor growth and are consistent with other tumor models.[55] Melatonin inhibits tumor production of 13-HODE by impeding cAMP-dependent LA uptake through melatonin receptors.[5,59] The current study supports previous findings that melatonin suppresses the Warburg effect in part by reducing 13-HODE formation. Furthermore, in our current study, the markedly increased inhibition of tumor growth in the bLAD groups can be attributed primarily to the rapid, early onset of the dark phase and prolonged duration of the nocturnal melatonin signal rather than to the elevated peak amplitude alone. This conclusion is supported by the fact that inhibition of hepatoma metabolism and proliferative activity by melatonin during acute tumor perfusion in situ saturates at 1 nM (232 pg/mL).[4] Nonetheless, other as-yet unknown melatonin-mediated mechanisms may also have been involved.

Without exception, all of the aforementioned parameters were significantly inhibited and to a greater extent in hepatomas in response to the altered spectral transmittance of bLAD compared with CWF lighting. Our previous studies showed that TFA concentrations in all of the major metabolic tissues (that is, liver, fat, heart, and muscle) were significantly lower in animals maintained under bLAD compared with CWF lighting conditions and paralleled the decrease in dietary intake exhibited by bLAD rats.[25] In addition, 7288CTC hepatoma, a highly undifferentiated, rapidly metabolizing tumor, displays a similar association in both TFA and LA levels and in overall lipid fraction content. Furthermore, we demonstrated that daily melatonin supplementation in rats bearing either rodent 7288CTC hepatoma or human MCF7 breast tumors results in lower overall tumor lipid content.[4] Therefore the markedly elevated and prolonged nocturnal melatonin levels most likely were responsible for the unusual tumor phenotype we observed in the bLAD-exposed hepatoma-bearing rats.

Light intensity, wavelength, duration, and timing are essential components in the regulation of mammalian circadian rhythms of physiology and metabolism. The nighttime circadian melatonin signal is a critical synchronizer, or internal zeitgeber, that is responsible for influencing circadian rhythms of metabolism and physiology in both normal and neoplastic tissues. The present investigation provides compelling evidence for the hypothesis that supraphysiologic levels of melatonin, as evinced in rats exposed to blue-enriched LED light during daytime, contributes to the enhanced inhibition of hepatoma metabolism, signaling activity, and growth. Additional studies in both rodents and human subjects are warranted to better understand the potentially beneficial effects of daytime blue-enriched LED light exposure and enhanced circadian nocturnal melatonin-associated inhibition of cancer.

Acknowledgments

This work was supported in part by a Tulane University School of Medicine and Louisiana Cancer Research Consortium Startup Grant (no. 631455 to DEB), NIH grant (National Cancer Institute no.

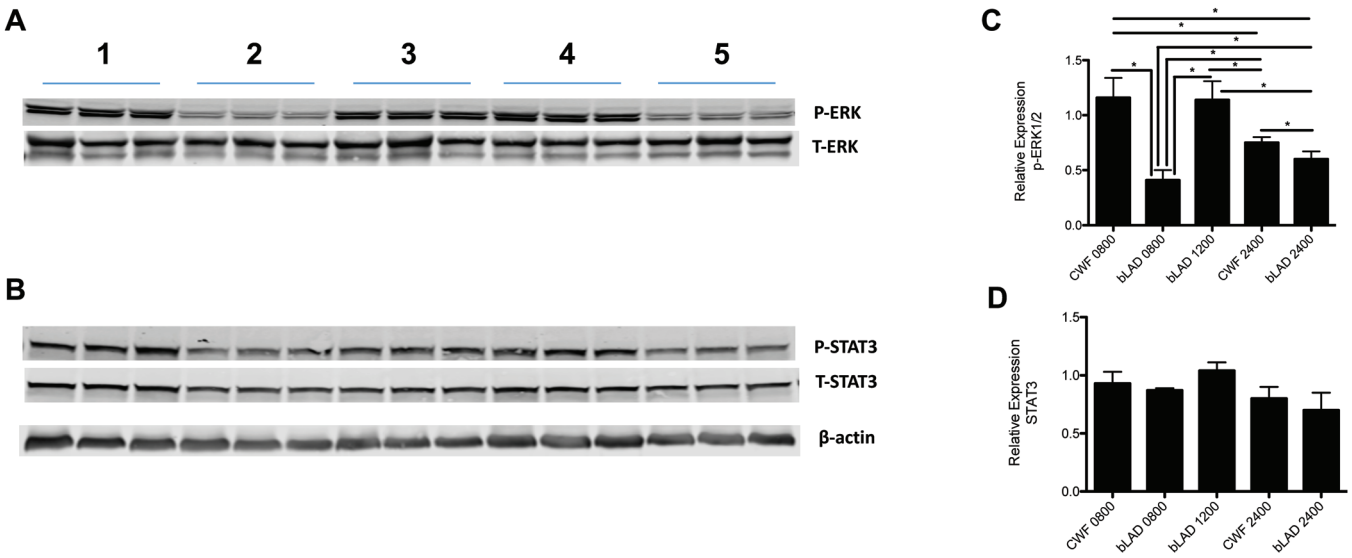

Figure 4. Western blot analysis of the expression of phosphorylated (p; upper panel) and total (lower panel) forms of (A) ERK 1/2 and (B) STAT3 in hepatomas of the control CWF group I (lane 1) at 0800, experimental bLAD group III at 0800 (lane 2), experimental bLAD group IV at 1200 (lane 3), control CWF group II at 2400 (lane 4), and experimental bLAD group V at 2400 (lane 5); each lane represents 3 tumors. Vertical bars represent the relative expression (mean ± 1 SD); derived from the densitometric quantitation of the immunoblots) in hepatomas of either (C) pERK1/2 or (D) pSTAT3. The relative expression of pERK1/2 represents the ratio of pERK1/2 protein to total (T) ERK1/2 protein; β-actin is shown as a loading control. *, Differences are significant ($P < 0.05$).

1R56CA193518-01 to SMH and DEB), and American Association for Laboratory Animal Science Grants for Laboratory Animal Science (GLAS) Award (to RTD and DEB). We acknowledge and are grateful for the technical support of Dr Georgina Dobek, Mrs Lee Barton, Ms Joy Ettling, Mr Adam N Danner, Ms Casey L Fiorella, Ms Alex M Johnson, and Mr Cary M Pfister.

References

1. **Altekruse SF, McGlynn KA, Reichman ME.** 2009. Hepatocellular carcinoma incidence, mortality and survival trends in the United States from 1975 to 2005. J Clin Oncol **27:**1485–1491. https://doi.org/10.1200/JCO.2008.20.7753.
2. **Altimus CM, Guler AD, Alam NM, Arman AC, Prusky GT, Sampath AP, Hattar S.** 2010. Rod photoreceptors drive circadian photoentrainment across a wide range of light intensities. Nat Neurosci **13:**1107–1112. https://doi.org/10.1038/nn.2617.
3. **Berson DM, Dunn FA, Takao M.** 2002. Phototransduction by retinal ganglion cells that set the circadian clock. Science **295:**1070–1073. https://doi.org/10.1126/science.1067262.
4. **Blask DE, Brainard GC, Dauchy RT, Hanifin JP, Davidson LK, Krause JA, Sauer LA, Rivera-Bermudez MA, Dubocovich ML, Jasser SA, Lynch DT, Rollag MD, Zalatan F.** 2005. Melatonin-depleted blood from premenopausal women exposed to light at night stimulates growth of human breast cancer xenografts in nude rats. Cancer Res **65:**11174–11184. https://doi.org/10.1158/0008-5472.CAN-05-1945.
5. **Blask DE, Dauchy RT, Dauchy EM, Mao L, Hill SM, Greene MW, Belancio VP, Sauer LA, Davidson LK.** 2014. Light exposure at night disrupts host/cancer circadian regulatory dynamics: impact on the Warburg effect, lipid signaling and tumor growth prevention. PLoS One **9:**1–14. https://doi.org/10.1371/journal.pone.0102776.
6. **Blask DE, Dauchy RT, Sauer LA, Krause JA.** 2004. Melatonin uptake and growth prevention in rat hepatoma 7288CTC in response to dietary melatonin: melatonin receptor-mediated inhibition of tumor linoleic acid metabolism to the growth signaling molecule 13-hydroxyoctadecadienoic acid and the potential role of phytomelatonin. Carcinogenesis **25:**951–960. https://doi.org/10.1093/carcin/bgh090.
7. **Brainard GC.** 1989. Illumination of laboratory animal quarters: participation of light irradiance and wavelength in the regulation of the neuroendocrine system. p 69–74. In: Guttman HN, Mench JA, Simmonds RC, editors. Science and animals: addressing contemporary issues, Greenbelt (MD): Scientists Center for Animal Welfare.
8. **Brainard GC, Hanifin JP.** 2005. Photons, clocks, and consciousness. J Biol Rhythms **20:**314–325. https://doi.org/10.1177/0748730405278951.
9. **Brainard GC, Hanifin JP, Rollag MD, Greeson JM, Byrne B, Glickman G, Gerner E, Sanford B.** 2001. Human melatonin regulation is not mediated by the 3 cone photopic visual system. J Clin Endocrinol Metab **86:**433–436. https://doi.org/10.1210/jcem.86.1.7277.
10. **Brainard GC, Richardson BA, King TS, Matthews SA, Reiter RJ.** 1983. The suppression of pineal melatonin content and N-acetyltransferase activity by different light irradiances in the Syrian hamster: a dose-response relationship. Endocrinology **113:**293–296. https://doi.org/10.1210/endo-113-1-293.
11. **Brainard GC, Richardson BA, King TS, Reiter RJ.** 1984. The influence of different light spectra on the suppression of pineal melatonin content in the Syrian hamster. Brain Res **294:**333–339. https://doi.org/10.1016/0006-8993(84)91045-X.
12. **Brainard GC, Vaughan MK, Reiter RJ.** 1986. Effect of light irradiance and wavelength on the Syrian hamster reproductive system. Endocrinology **119:**648–654. https://doi.org/10.1210/endo-119-2-648.
13. **Commission International de L'Eclairage.** 2004. Ocular lighting effects on human physiology and behavior. p 1–54. CIE Publication; no. 158, Vienna (Austraia): CIE. http://doi.org/10.4224/20377921
14. **Demaria M, Poli B.** 2012. PMK2, STAT2 and HIF1α: The Warburg's viscious circle. JAKSTAT **1:**194–196. https://doi.org/10.4161/jkst.20662.
15. **Dacey DM, Liao HW, Peterson BB, Robinson FR, Smith VC, Pokorny J, Yau KY, Gamlin PD.** 2005. Melanopsin-expressing ganglion cells in primate retina signal colour and irradiance and project to the LGN. Nature **433:**749–754. https://doi.org/10.1038/nature03387.
16. **Dauchy RT, Blask DE, Sauer LA, Brainard GC, Krause JA.** 1999. Dim light during darkness stimulated tumor progression by enhancing tumor fatty acid uptake and metabolism. Cancer Lett **144:**131–136. https://doi.org/10.1016/S0304-3835(99)00207-4.
17. **Dauchy RT, Dauchy EM, Hanifin JP, Gauthreaux SL, Mao L, Beleancio VP, Ooms TG, Dupepe LM, Jablonski MR, Warfield B, Wren MA, Brainard GC, Hill SM, Blask DE.** 2013. Effects of spectral transmittance through standard laboratory cages on circadian metabolism and physiology in nude rats. J Am Assoc Lab Anim Sci **52:**146–156.

18. **Dauchy RT, Dauchy EM, Tirrell RP, Hill CR, Davidson LK, Greene MW, Tirrell PC, Wu J, Sauer LA, Blask DE.** 2010. Dark-phase light contamination disrupts circadian rhythms in plasma measures of physiology and metabolism in rats. Comp Med **60:**348–356.
19. **Dauchy RT, Dupepe LM, Ooms TG, Dauchy EM, Hill CR, Mao L, Belancio VP, Slakey LM, Hill SM, Blask DE.** 2011. Eliminating animal facility light-at-night contamination and its effect on circadian regulation of rodent physiology, tumor growth and metabolism: A challenge in the relocation of a cancer research laboratory. J Am Assoc Lab Anim Sci **50:**326–336.
20. **Dauchy RT, Sauer LA.** 1986. Preparation of "tissue-isolated rat tumors for perfusion: a new surgical technique that preserves continuous blood flow. Lab Anim Sci **36:**678–681.
21. **Dauchy RT, Dauchy EM, Mao L, Belancio VP, Hill SM, Blask DE.** 2012. A new apparatus and surgical technique for the dual perfusion of human tumor xenografts in situ in nude rats. Comp Med **62:**99–108.
22. **Dauchy RT, Wren MA, Dauchy EM, Hanifin JP, Jablonski MR, Warfield B, Brainard GC, Hill SM, Mao L, Dupepe LM, Ooms TG, Blask DE.** 2013. Effects of spectral transmittance through red-tinted cages on circadian metabolism and physiology in nude rats. J Am Assoc Lab Anim Sci **52:**745–755.
23. **Dauchy RT, Xiang S, Mao L, Brimer S, Wren MA, Yuan L, Anbalagan M, Hauch A, Frasch T, Rowan BG, Blask DE, Hill SM.** 2014. Circadian and melatonin disruption by exposure to light at night drives intrinsic resistance to tamoxifen therapy in breast cancer. Cancer Res **74:**4099–4110. https://doi.org/10.1158/0008-5472.CAN-13-3156.
24. **Dauchy RT, Hoffman AE, Wren-Dail MA, Hanifin JP, Warfield B, Brainard GC, Xiang S, Yuan L, Hill SM, Belancio VP, Dauchy EM, Smith K, Blask DE.** 2015. Daytime blue light enhances the nighttime circadian melatonin inhibition of human prostate cancer growth. Comp Med **65:**473–485.
25. **Dauchy RT, Wren-Dail MA, Hoffman AE, Hanifin JP, Warfield B, Brainard GC, Hill SM, Belancio VP, Dauchy EM, Blask DE.** 2016. Effects of daytime exposure to light from blue-enriched light-emitting diodes light the nighttime melatonin amplitude and circadian regulation of rodent metabolism and physiology. Comp Med **66:**373–383.
26. **Davis S, Mirick DK, Stevens RG.** 2001. Night shift work, light at night, and the risk of breast cancer. J Natl Cancer Inst **93:**1557–1562. https://doi.org/10.1093/jnci/93.20.1557.
27. **Diaz B, Blazquez E.** 1986. Effect of pinealectomy on plasma glucose, insulin, and glucagon levels in the rat. Horm Metab Res **18:**225–229. https://doi.org/10.1055/s-2007-1012279.
28. **Ge D, Dauchy RT, Liu S, Zhang Q, Mao L, Dauchy EM, Blask DE, Hill SM, Rowan BG, Brainard GC, Hanifin JP, Cecil KS, Xiong Z, Myers L, You Z.** 2013. Insulin and IGF1 enhance IL17-induced chemokine expression through a GSK3B-dependent mechanism: a new target for melatonin's antiimflammatory action. J Pineal Res **55:**377–387.
29. **Ecker JL, Dumitrescu ON, Wong KY, Alam NM, Chen SK, LeGates T, Renna JM, Prusky GT, Berson DM, Hattar S.** 2010. Melanopsin-expressing retinal ganglion-cell photoreceptors: cellular diversity and role in pattern vision. Neuron **67:**49–60. https://doi.org/10.1016/j.neuron.2010.05.023.
30. **Fonken LK, Nelson RJ.** 2014. The effects of light at night on circadian clocks and metabolism. Endocr Rev **35:**648–670. https://doi.org/10.1210/er.2013-1051.
31. **Gabel V, Maire M, Chellappa CF, Reichert SL, Schmidt C, Hommes V, Viola AU, Cajochen C.** 2013. Effects of artificial dawn and morning blue light on daytime cognitive performance, wellbeing, cortisol, and melatonin levels. Chronobiol Int **30:**988–997. doi:https://www.tandfonline.com/doi/full/10.3109/07420528.2013.793196.
32. **Gooley JJ, Rajaratnam SM, Brainard GC, Kronauer RE, Czeisler CA, Lockley SW.** 2010. Spectral responses of the human circadian system depend on the irradiance and duration of exposure to light. Sci Transl Med **2:**31ra33. https://doi.org/10.1126/scitranslmed.3000741.
33. **Gough DJ, Koetz L, Levy DE.** 2013. The MEK-ERK pathway is necessary for serine phosphorylation of mitochondrial STAT3 and Ras-mediated transformation. PLoS One **8:**1–9. https://doi.org/10.1371/journal.pone.0083395.Correction: The MEK-ERK pathway is necessary for serine phosphorylation of mitochondrial STAT3 and Ras-mediated transformation. PLoS ONE **8:** 10.1371/annotation/5b4e222a-a9bc-4036-882e-cd975301ca89. https://doi.org/10.1371/annotation/5b4e222a-a9bc-4036-882e-cd975301ca89
34. **Hansen J.** 2001. Increased breast cancer risk among women who work predominantly at night. Epidemiology **12:**74–77. https://doi.org/10.1097/00001648-200101000-00013.
35. **Hattar S, Lucas RJ, Mrosovsky N, Thompson S, Douglas RH, Hankins MW, Lem J, Biel M, Hofmann F, Foster RG, Yau KW.** 2003. Melanopsin and rod-cone photoreceptive systems account for all major accessory visual functions in mice photosensitivity. Nature **424:**76–81.
36. **Heeke DS, White MP, Mele GD, Hanifin JP, Brainard GC, Rollage MD, Winget CM, Holley DC.** 1999. Light-emitting diodes and cool white fluorescent light similarly suppress pineal gland melatonin and maintain retinal function and morphology in the rat. Lab Anim Sci **49:**297–304.
37. **Howlader N, Noone AM, Krapcho M, Miller D, Bishop K, Altekruse SF, Kosary CL, Yu M, Ruhl J, Tatalovich Z, Mariotto A, Lewis DR, Chen HS, Feuer EJ, Cronin KA, editors.** 2016. SEER cancer statistics review, 1975–2013. Bethesda (MD): National Cancer Institute.
38. **Hughes ME, Hogenesch JB, Kornacker K.** 2010. JKT_CYCLE: and efficient nonparametric algorithm for detecting rhythmic components in genome-scale data sets. J Biol Rhythms **25:**372–380. https://doi.org/10.1177/0748730410379711.
39. **Illnerová H, Vanecek J, Hoffman K.** 1983. Regulation of the pineal melatonin concentration in the rat (*Rattus norvegicus*) and the Djungarian hamster (*Phodopus sungorus*). Comp Biochem Physiol A Comp Physiol **74:**155–159. https://doi.org/10.1016/0300-9629(83)90727-2.
40. **Institute for Laboratory Animal Research.** 2011. Guide for the care and use of laboratory animals, 8th ed. Washington (DC): National Academies Press.
41. **Illuminating Engineering Society of North America.** 2008. Light and human health: An overview of the impact of optical radiation on visual, circadian, neuroendocrine, and neurobehavioral responses, IED TM-18-08. New York (NY): Illuminating Engineering Society of North America
42. **Jasser SA, Hanifin JP, Rollag MD, Brainard GC.** 2006. Dim light adaptation attenuates acute melatonin suppression in humans. J Biol Rhythms **21:**394–404. https://doi.org/10.1177/0748730406292391.
43. **Kalsbeek A, Strubbe JH.** 1998. Circadian control of insulin secretion is independent of the temporal distribution of feeding. Physiol Behav **63:**553–558. https://doi.org/10.1016/S0031-9384(97)00493-9.
44. **Kennaway DJ, Voultsios A, Varcoe TJ, Moyer RW.** 2002. Melatonin in mice: rhythms, response to light, adrenergic stimulation, and metabolism. Am J Physiol Regul Integr Comp Physiol **282:**R358–R365. https://doi.org/10.1152/ajpregu.00360.2001.
45. **Klein DC, Weller JL.** 1972. Rapid light-induced decrease in pineal serotonin N-acetyltransferase activity. Science **177:**532–533. https://doi.org/10.1126/science.177.4048.532.
46. **Kubo T, Ozasa K, Mikami K, Wakai K, Fujino Y, Watanabe Y, Miki T, Nakao M, Hayashi K, Suzuki K, Mori M, Washio M, Sakauchi F, Ito Y, Yoshimura T, Tamakoshi A.** 2006. Prospective cohort study of the risk of prostate cancer among rotating-shift workers: findings from the Japan collaborative cohort study. Am J Epidemiol **164:**549–555. https://doi.org/10.1093/aje/kwj232.
47. **Laakso ML, Porkka-Heiskane T, Alila A, Peder M, Johansson G.** 1988. Twenty-four-hour patterns of pineal melatonin and pituitary and plasma prolactin in male rats under 'natural' and artificial lighting conditions. Neuroendocrinol **48:**308–313. https://doi.org/10.1159/000125027
48. **Lima FB, Machado UF, Bartol I, Seraphim PM, Sumida DH, Moraes SMF, Hell NS, Okamotot NM, Saad MJ, Carvalho CR, Cipolla-Neto J.** 1998. Pinealectomy causes glucose intolerance and decreases adipose cell responsiveness to insulin in rats. Am J Physiol **275:**E934–E941.
49. **Lucas RJ, Pierson SN, Berson DM, Brown TM, Cooper HM, Czeisler CA, Figueiro MG, Gamlin PD, Lockely SW, O'Hagan JB, Price LLA, Provencio I, Skene DJ, Brainard GC.** 2014. Measuring and using light in the melanopsin age. Trends Neurosci **37:**1–9. https://doi.org/10.1016/j.tins.2013.10.004.
50. **Moore RY, Lenn NJ.** 1972. A retinohypothalamic projection in the rat. J Comp Neurol **146:**1–14. https://doi.org/10.1002/cne.901460102.

51. **Nelson DL, Cox NM.** 2005. Hormonal regulation of and integration of mammalian metabolism, Chapter 23. p 881–992. In: Lehninger principles of biochemistry; New York (NY): WH Freeman.
52. **Neufield Department of Clinical Neurosciences Medical Sciences Division.** [Internet]. 2016. Rodent Toolbox v1.xlsx. [Cited 05 November, 2017]. Available at: https//www.ndcn.ox.ac.uk/team/stuart-peirson/downloadstile-14/filetile-21/@@download
53. **Panda S, Provencio I, Tu DC, Pires SS, Rollag MD, Csatrucci AM, Pletcher MT, Sato TK, Wiltshire T, Andahazy M, Kay SA, Van Gelder RN, Hogenesch JB.** 2003. Melanopsin is required for nonimage-forming photic responses in blind mice. Science **301:**525–527. https://doi.org/10.1126/science.1086179.
54. **Reiter RJ.** 1991. Pineal gland: interface between photoperiodic environment and the endocrine system. Trends Endocrinol Metab **2:**13–19. https://doi.org/10.1016/1043-2760(91)90055-R.
55. **Reiter RJ, Rosales-Corral SA, Tan DX, Acna-Castroviejo D, Qin L, Yang SF, Xu K.** 2017. Melatonin, a full service anti-cancer agent: inhibition of initiation, progression, and metastasis. Int J Mol Sci **18:**843–887. https://doi.org/10.3390/ijms18040843.
56. **Sauer LA, Stayman JW 3rd, Dauchy RT.** 1982. Amino acid, glucose, and lactic acid utilization by rat tumors. Cancer Res **42:**4090–4097.
57. **Sauer LA, Dauchy RT.** 1988. Identification of linoleic and arachidonic acids as the factors in hyperlipemic blood that increases [^{3}H] thymidine incorporation in hepatoma 7288CTC perfused in situ. Cancer Res **48:**3106–3111.
58. **Sauer LA, Dauchy RT, Blask DE, Armstrong BJ, Scalici S.** 1999. 13-Hydroxyoctadecadienoic acid is the mitogenic signal for linoleic acid-dependent growth of rat hepatoma 7288ctc in vivo. Cancer Res **59:**4688–4692.
59. **Schernhammer ES, Laden F, Speizer FE, Willett WC, Hunter DJ, Kawachi I, Colditz GA.** 2001. Rotating night shifts and risk of breast cancer in women participating in the nurses' health study. J Natl Cancer Inst **93:**1563–1568. https://doi.org/10.1093/jnci/93.20.1563.
60. **Stevens RG, Brainard GC, Blask DE, Lockley SW, Motta ME.** 2013. Breast cancer and circadian disruption from electric lighting in the modern world. CA Cancer J Clin **64:**207–218. https://doi.org/10.3322/caac.21218.
61. **Weng S, Estevez ME, Berson DM.** 2013. Mouse ganglion-cell photoreceptors are driven by the most sensitive rod pathway and by both types of cones. PLoS One **8:**1–13. https://doi.org/10.1371/journal.pone.0066480.
62. **Wolden-Hanson T.** 2010. Changes in body composition in response to challenges during aging in rats. p 64–83. In: Mobbs CV, Hof PR, editors. Body composition and aging. vol. 37. New York (NY): Karger, Basil.
63. **Wolden-Hanson T, Mitton DR, McCants RL, Yellon SM, Wilkinson CW, Matsumoto AM, Rasmussen DD.** 2000. Daily melatonin administration to middle-aged rats suppresses body weight, intraabdominal adiposity, plasma leptin and insulin independent of food intake and total body fat. Endocrinology **141:**487–497. https://doi.org/10.1210/endo.141.2.7311.
64. **Wren MA, Dauchy RT, Hanifin JP, Jablonski MR, Warfield B, Brainard GC, Blask DE, Hill SM, Ooms TG, Bohm RP Jr.** 2014. Effect of different spectral transmittances through tinted animal cages on circadian metabolism and physiology in Sprague–Dawley rats. J Am Assoc Lab Anim Sci **53:**44–51.